Rev. Adv. Mater. Sci. 36 (2014) 40-61

CARBON NANOTUBES BASED THIN FILMS: FABRICATION, CHARACTERIZATION AND APPLICATIONS

L. Fu[1] and A. M. Yu[1,2]

[1]Faculty of Life and Social Sciences, Swinburne University of Technology, Hawthorn VIC 3122, Australia
[2]College of Chemical and Environmental Engineering, Hubei Normal University, 435002, China

Received: May 25, 2013

Abstract. Composite thin films based on carbon nanotubes have received immense attention which is attributed to their distinct mechanical, thermal, optical and structure properties. Depending on the film compositions and preparation methods, carbon nanotube based thin films can be tuned for various applications in many fields. In this comprehensive review paper, we overview the recent methods for the fabrication of carbon nanotube based thin films and the versatile techniques for film characterization. Applications of carbon nanotube based thin films and their devices are also reviewed. The remaining issues that impede the practical applications of thin films are pointed out to enlighten their future research.

1. INTRODUCTION

Carbon nanotubes (CNTs) have triggered enormous world-wide interest since it was discovered in 1991 by Iijima [1]. CNTs are built from sp2 carbon units and present a seamless structure with hexagonal honeycomb lattices [1,2]. Basically, there are two types of CNTs: Single-walled carbon nanotubes (SWCNTs) and multi-walled carbon nanotubes (MWCNTs) [1-3]. SWCNTs are single graphene rolls with diameters of 0.8 to a few nanometers while MWCNTs are concentric grapheme tubes that can have diameters from a few to more than a hundred nanometers. Many theoretical and experimental works have revealed the outstanding properties of CNTs. Their stiffness and strength are phenomenal. Experimental results shows that CNTs have the Young's modulus of approximately 1 TPa [4,5]. For comparison, the stiffest conventional carbon fibres and glass fibres have Young's modulus of 800 GPa and 70 GPa, respectively. The electrical properties of CNTs are depended on the arrangement of the graphene. They could be either semiconductors or excellent conductors which have conductivity 1000 times to the copper [6]. Moreover, the thermal conductivity of an individual nanotube can reach 3500 W $m^{-1}K^{-1}$ [7,8]. Due to their unique mechanical, electrical, and thermal properties, CNTs have emerged as novel nanometric materials which have promising applications in many areas.

CNTs-related commercial activity has grown substantially during the past decade. Recently, 2D networks of CNT incorporated thin films, either CNTs in random networks, aligned arrays or anything in between, have attracted a great deal of attention. For example, 2D conductive CNT films display excellent mechanical flexibility, stretchability, and optical transparence. Such films have been used for conductive electrodes, and as artificial muscles [9]. The 3D aligned CNT arrays with properly engineered surfaces have been explored as dry adhesive tapes or biomimic gecko feet [10,11]. Incorporating other functional materials with CNTs could either improve the film property or greatly extend the range of application, such as battery electrodes, field emitter, antifouling films, antimicrobial, nanoelectronics and nanoscale sensors.

Corresponding author: A.M. Yu, e-mail: aiminyu@swin.edu.au

In this review, we begin by describing the various common fabrication techniques for preparing CNTs based thin films. We then highlight the established experimental techniques for characterization of CNTs based thin films, exposing an array of its unique properties. Finally, we discuss how each particular property can be exploited for potential applications.

2. FABRICATION METHODS FOR PREPARING CARBON NANOTUBE BASED THIN FILMS

CNTs based thin films have been prepared by various techniques. In this section, we will focus on introducing common techniques for coating and decorating CNTs films. Last but not least, direct film growth using chemical vapor deposition (CVD) is also discussed.

2.1. Spray-coating

Spray-coating involves spraying CNTs dispersion onto a heated substrate where every sprayed droplet reaches the hot substrate surface and undergoes pyrolytic decomposition, consequently forms a thin layer of CNTs film. The excess solvent and byproducts escape to the air through the vapor phase. The major advantage of spray-coating process is the ability of forming large area and thick films. Various substrates can be used for spray-coating CNTs including glass, quartz, silicon wafer, ITO, FTO which made this method suitable for a large range of device fabrication [12].

Surfactants such as sodium dodecyl sulfate (SDS) [13] and sodium dodecylbenzene sulfonate (SDBS) [14] are commonly added to form uniform CNTs water dispersion to be used in the spraycoating process. Another approach to form well dispersed CNTs is to disperse CNTs into organic solvents such as anhydrous ethanol. Low speed centrifugation is usually carried out after the dispersion procedure to separate the bundles as sediments. It is worth nothing that the stability of the thin film made by spray-coating method is strongly affected by the substrate used. Films are easy to peel off when the nanotube adhesion to substrate is weak. In this case, substrates could be modified to enhance the interaction with CNTs. Schindler *et al.* [13] recently demonstrated that coating a layer of polyimide or 3-aminopropyl triethoxysilan by self-assembly on glass substrate prior to CNTs deposition could increase the sheet resistance by 10%. This pre-coating also facilitates the evaporation of solvent. Surface treatment was also employed to increase the conductivity of films. For example, 70% HNO_3 treatment removes the surfactants from the CNTs surface resulting in the increase in inter-tube conductance. 99% $SOCl_2$ treatment has the effect of doping on the CNTs surface, which enhance the overall conductance of the film.

Two basic strategies are employed to prepare CNTs based composite films by spray-coating method. A one-step molding process that gives well-formed morphology, involves using a pre-mixed solution of dispersed CNTs and the aqueous solution of incorporated material. On the other hand, depositing CNTs and material separately by spray-coating technique is the secondary way to form CNTs based composite films due to the difference in densities and sizes between two materials.

2.2. Dip-coating

Dip-coating is a facile solution based surface coating method providing great potential to scale up for largescale coating and does not require sophisticated apparatus. Essentially, the substrate is immersed into the CNTs based dispersion at a constant speed and remains inside for a period of time then starts to be pulled up. The pull up process needs a constant speed on carrying out to avoid any jitters. A thin layer of dispersion will be picked-up with the substrate and a thin film forms after the drying process (Fig. 1a). The amount of captured dispersion depends on several factors: the dispersion viscosity, immersion time, pull-up speed (usually faster withdrawal gives thicker coating layer) and the interaction between the dispersion and substrate. The quality of the thin film is also affected by the drying process. One drawback of the dip-coating technique is that the fabrication process occurs at both sides of the substrate, which may restrict its application.

The simple operation process has been used for fabricating CNTs/polymer composite films. Li *et al.* [15] reported the utilization of dip coating method for fabricating transparent and conductive SWCNTs/polyvinyl butyral (PVB) composite film. The thickness of the SWCNTs/PVB composite film can be tuned by varying the concentration and quantity of SWCNTs/PVB ethanol dispersion. Other polymers like polystyrene, polyurethane elastomers [16] and poly(methyl methacrylate) (PMMA) [17], were also used for forming thin films with CNTs using the dip-coating method.

Introducing surfactants such as Triton X-100 and SDS would improve the dispersibility of CNTs for

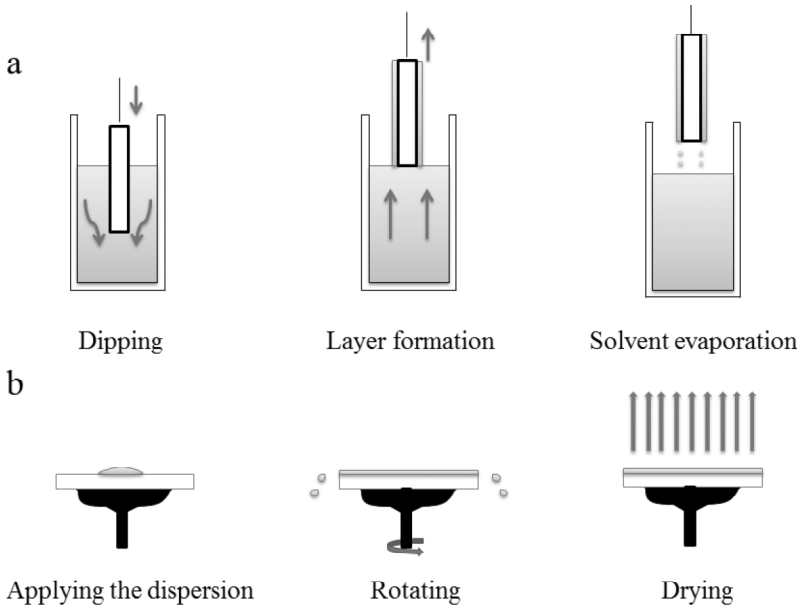

Fig. 1. Schematic diagrams of thin film preparation using (a) dip-coating and (b) spin-coating.

dip-coating. To improve the adhesion between substrate and film, pretreatment of substrate is necessary. Aminopropyltriethoxysilane is usually used for substrate treatment as an adhesion promoter by forming an interlayer between CNTs and substrate.

2.3. Spin-coating

Fabrication of CNTs based thin films using spincoating method involves depositing a small puddle of CNTs based dispersion onto the center of a substrate, then spinning the substrate to high speed allowing dispersion to spread and cover the substrate to form a thin film by centrifugal force (Fig. 1b).

The thickness of film normally relates with the dispersion viscosity, angular speed and spin time. The orientation of CNTs appeared to have an angle of approximately 45 °C relative to the radial direction of the film, which is independent on the spin rare and radial position [18]. The morphology of the thin film is also highly affected by the concentration of CNTs [19]. AFM study showed if SWCNTs concentration in blended solution is more than 2 wt.%, there is no interconnected phase separation microstructure and no island phase separation appeared on the film; the carbon nanotubes tend to aggregate. If the SWCNTs concentration equals to 1 wt.%, the interpenetrating network phase separation microstructure can be formed. Nevertheless, when the concentration drops below 0.5 wt.%, result would only show island phase separation microstructure.

Similar with dip-coating process, spin-coating is also a good method for preparing CNTs-polymer composite films. The addition of surfactant to enhance the dispersibility is the common strategy during the spin-coating procedure as well. However, the strong charge repulsion between complexes of CNTs and surfactant would prohibit CNTs deposition onto the substrate. To overcome this problem, three methods have been proposed. Yim *et al*. [20] prepared SWCNTs thin films without surfactant using multiple spin-coating. Meitl *et al.* [21] employed dual spinning to allow SWCNTs to land on the surface before they meet in dispersion, resulting in a film of individual SWCNTs. This method can achieve a desired film thickness without having charge repulsion between the tube-surfactant complexes. The third method is replacing conventional surfactants by amphiphilic surfactants. Pluronic and Triton-X are two commercial non-ionic surfactants introduced to the CNTs based dispersion. Jo *et al*. [22] recently reported the use of a lower molecular weight (~2000 g/mol) non-inoic surfactant, quinquethiophene terminated poly(ethylene glycol), which can be easily washed out after deposition.

There exist a few drawbacks of spin-coating technique. Firstly, spin-coating is not suitable for large-scale coating because large substrates cannot be spun at a sufficiently high rate to form a uniform layer. Secondly, the non-uniform distribution of materials along the radial direction becomes worst when scaling up the dimension. In addition, for multilayer film fabrication, the multiple spin coating process is too cumbersome. Last but not least, the spin-coat-

ing method lacks material efficiency. In a typical deposit process, most material is flung off and disposed.

2.4. Sol-gel method

The sol-gel process is a wet-chemical technique widely used for the fabrication of metal oxides materials. The underlying principal of sol-gel method is the transition of a system from a colloidal sol into a solid gel phase. Typically, a solution of the appropriate precursors is formed first, followed by conversing into gel state by hydrolysis and condensation. Sol-gel has been used to incorporate CNTs into different matrix with the merits of easier composition control, better homogeneity, non-vacuum process, low processing temperature and low cost equipment required. Synthesized precursor solution can be deposited onto substrate by spincoating, dip-coating or spray-coating methods and pyrolyzed at a low temperature. Extra steps of drying and subsequent calcinations of the gel are usually carried out for densification of films and burn out organic residues coming from the solution. CNTs-SiO_2 and CNTs-TiO_2 thin films are considered as the two most successful films fabricated by sol-gel technique.

Eq. (1) represents the common sol-gel process to form SiO_2 thin film (using silica alkoxydes as starting materials), in which R is an alkyl group. Eqs. (2) and (3) represent the hydrolysis and condensation steps of monomeric alkoxysilanes respectively.

$$Si(OR)_4 + (4-x)H_2O \rightarrow SiO_x(OH)_{4-2x} + 4ROH, \quad (1)$$

$$Si\text{-}OR + H_2O \rightarrow Si\text{-}OH + ROH, \quad (2)$$

$$Si\text{-}OR + HO\text{-}Si \rightarrow Si\text{-}O + ROH. \quad (3)$$

Introducing CNTs into the sol preparation is the first step of fabrication of CNTs-SiO_2 thin films through the sol-gel method. The most widely-used precursors for silica resource are tetramethoxysilane (TMOS) and tetraethoxysilane (TEOS). The sol preparation is simply mixing precursors with water, co-solvent and CNT. The co-solvent is usually methanol or ethanol, for adjusting viscosity of the sol and controlling the thickness of the produced thin films. Acidic and basic catalysts are usually added to accelerate the hydrolysis and condensation process. Berguiga *et al*. [23] have shown that high quality CNTs-SiO_2 thin film can be fabricated by mixing TEOS with HCl, ethanol and functionalized MWCNTs followed by sonification. The molar ratio between Si of SiO_2 matrix and C of MWCNTs is 7.5. Films were deposited by the dip coating method on pre-cleaned glass substrate then annealed for 20 min at 350 °C. The fabrication method of CNTs-TiO_2 is very similar to CNTs-SiO_2. The sol solution contains the mixture of titanium butoxide, water, HCl, and ethanol. Thin films were formed by dipping the substrate into the sol for a few minutes then withdrawn vertically. Films can be thickened by multiple dipping [24-26]. Beyond that, sol-gel method is also appropriate for incorporating CNTs with other material such as Al_2O_3 [27], NiO [28,] and WO_3 [29].

2.5. Vacuum filtration

Vacuum filtration is a simple method to separate CNTs composites from solvents and compact into films which is achieved based on the different pressures between two sides Buchner funnel. The thin film formed is then peeled off from the filter paper and subjected to drying process.

Luo *et al.* [30] were the first to use this approach to fabricate CNTs/Nafion composite films which exhibited high conductivity and superhydrophobicity. The wettability of the composite film could be controlled by varying the filtering rate and the content ratio between two substances. Functionalization of CNTs was also achieved by vacuum filtration. Yao *et al.* [31] used octadecylamine for amination of MWCNTs by vacuum filtration method. Introducing different types of CNTs into vacuum filtration system could accomplish film delamination. In addition, placing metal mash or metal mask above the filter paperallows the formation of a particular pattern for different applications.

Despite the aforesaid advantages, the thin films made by vacuum filtration are usually quite thick, thus may not be preferred for certain applications. Furthermore, film transfer is necessary as the peeled film could not be directly used for device applications.

2.6. Electrophoretic deposition (EPD)

Electrophoretic deposition (EPD) occurs when charged particles from a colloidal dispersion move towards an electrode under the constant electric field. Charged CNTs accumulate at the electrode during the EPD processes to form a homogeneous and rigid film. One major limitation of EPD is the deposition only occurs on conductive surface. Fig. 2a shows the schematic diagram of electrophoretic deposition of a CNTs film. The surfactant wrapped CNTs possess a negative surface charge.

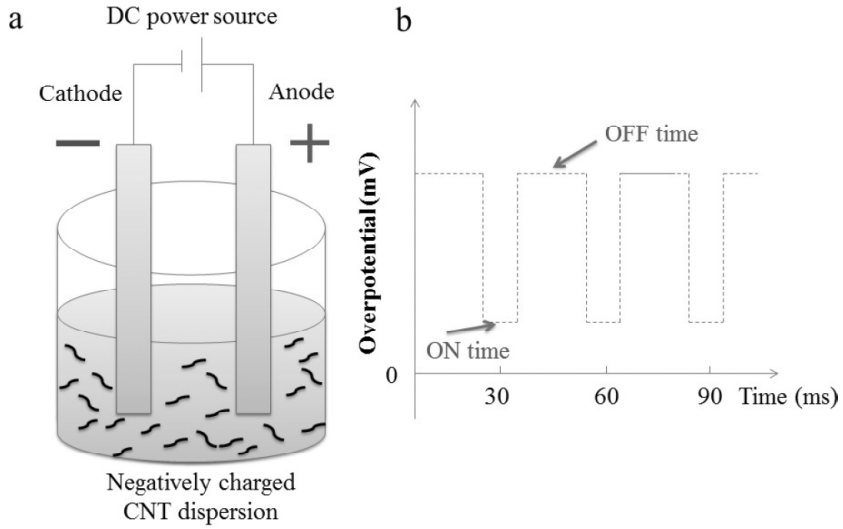

Fig. 2. (a) Schematic diagram of electrophoretic deposition of a CNT film. (b) A typical pulse-potential waveform.

The first report on depositing CNTs by EPD method was from Du *et al.* [32]. They deposited MWCNTs from ethanol/acetone dispersion onto a metallic substrate and observed hydrogen evolution on the cathode, which led to a porous structure of the film. Additional EPD after CNTs film deposition can be employed to deposit nanoparticles into CNTs film structure or to form a new layer. Alternatively, CNTs composite films can be obtained by EPD from stable dispersions containing two or more substances. The components could also be pre-assembled to form building blocks in the dispersion before EPD. Zhang *et al*. [33] reported the deposition of MnO_2-coated CNTs on a flexible graphite sheet (FGS). MnO_2 was firstly deposited onto CNTs by microwave heating method followed by depositing the compound onto FGS through EPD method. To improve the adhesion of CNTs to substrate and increase the deposition rate, charger salts are usually introduced to the dispersion. The type of salts used determines where (anode or cathode) the deposition occurs. As an example, CNTs will be deposited onto cathode when the dispersion contains quaternary ammonium salt and NaOH while CNTs will be deposited at anode when metal salts are used. This migration and subsequent deposition of CNTs is attributed to the preferential adsorption of ions in the solution by the CNTs [34].

2.7. Pulse electrodeposition

Pulse electrodeposition involves alternating swiftly potential or current to produce a series of pulses of equal amplitude, duration and polarity, separated by zero current. Fig. 2b shows the typical pulsepotential waveform. Each circle of pulse consists of an ON-time and OFF-time during the potential or current applied and zero current applied respectively. The OFF-time during the pulse electrodeposition discharges the negatively charged layer and allows the ions to diffuse toward the substrate. This method allows synthesis of coatings with controlled thickness as well as composition by regulating pulse parameters. It is also able to co-deposit nano and micron sized metal particles onto existing films.

Various metals and metallic oxides have been incorporated with CNTs to form composite films by pulse electrodeposition technique. Su *et al.* [35] demonstrated that MWCNTs/Co films could be synthesized bypulse reverse current (PRC) electrodeposition from aqueous bath containing cobalt sulfate and MWCNTs. Comparing with DC electrodeposition, the composite produced by PRC electrodeposition displays higher hardness and better resistance to wear and corrosion properties. A relatively thin and uniform coverage of amorphous RuO_2-H_2O nanoparticle layer on CNTs could be obtained by pulse potential electrochemical deposition [36]. The pulse potential cycle has the advantage of being capable of controlling the nucleation and growth of crystalline RuO_2 particles. Our group recently reported the deposition of Ag nanoparticles onto to MWCNTs/poly(dimethyldiallylammo-nium chloride) (PDDA) multilayer thin film from AgNO3 solution using a potentiostatic double pulse deposition method [37]. The size, density and morphology of Ag nanoparticles were well controlled by the pulse parameters. Ag particle of 10-500 nm with varied density could be electro-generated on MWCNTs/

PDDA surface when a voltage pulse of -600 mV for particle nucleation and -105 mV for growth were applied. The resulting composite film exhibited excellent electrocatalytic activity for the reduction of hydrogen peroxide.

2.8. Sputter deposition

Sputter deposition is a physical vapor deposition method widely used for deposition of certain materials onto existing CNTs film to form composite film. The underlying mechanism can be described as plasma ions (commonly use argon) hit the target with a high energy and consequently atoms are ejected from the surface of a target material and being deposited onto CNTs film. Controlled thin layer can be achieved by sputter elements, alloys, and compounds onto CNTs film. The disadvantage is the deposition is time consuming compared with other methods.

Depositing metal or metal oxide nanoparticles onto CNTs films have been found a number of applications in different fields. Au, Ag, and Pt nanoparticles were deposited at the tips and on the sidewalls of CNTs by magnetron sputtering performed satisfying electrochemical and electrocatalytic properties [38-40]. Formation of CNTs with Ni could also be prepared by sputtering deposition followed by annealing treatment in an NH_3 environment, which could be a more cost effective alternative for forming non-precious metal catalysts [41]. CNTs covered with 100 nm BaO/SrO layer has shown significant improvement in both field and thermionic emission (compared with pure CNTs film, field emission increased by a factor of two, the thermionic emission increased by more than four orders) [42]. Sputtering TiO_2 onto CNTs thin film then heated at certain degree can form anatase phase CNTs/TiO_2 composite films which showed a considerable photocatalytic activity [43].

2.9. Layer-by-layer (LbL) selfassembly

LbL self-assembly technique allows alternate deposition of complementary species on a substrate by exploiting electrostatic, hydrogen bonding or covalent bonding interactions. Different layers in the thin film overlaps and interpenetrates with adjacent layers. There are many species capable for deposition including polyelectrolytes, nanoparticles, proteins, enzymes, and many more.

CNTs cannot directly assemble with other materials in a water solution to form LbL films unless its surface has been appropriate functionalized. The fabrication process generally involves two steps. Firstly, CNTs need to be charged either by strong acids oxidation or wrapped by a polyelectrolyte, subsequently alternating adsorption with opposite charged species to generate films. Our group used poly(sodium 4-styrene-sulfonate) (PSS) to wrap CNTs, to form negatively surface charged PSS-CNTs dispersion then alternating absorption with PDDA to generated CNTs/polyelectrolyte multilayer thin film [44,45]. For the purpose of forming high quality polyelectrolyte wrapped CNTs dispersion and improves the loading rate during the LbL selfassembly process, acid pre-treatment of CNTs is usually carried out during the fabrication process. Wang and coworker [46] recently illustrated MWCNT pre-treatment using 5-aminoisophthalic acid to enhance the dispersibility during the fabrication MWCNTs/poly(p-xylylviologen) (PXV) thin film by LbL self-assembly technique. On the other hand, the surface oxidation inevitably changes the electronic properties of CNTs by disrupting their conjugated structure. Although high temperature hydrogen treatment shows the ability to reduce the oxidized bonds in treated-CNTs, but it cannot fully recover the properties of pristine CNTs [47]. To overcome these problems, Tettey *et al.* introduced a charge-inducing agent, aerosol OT (AOT), into this system. The AOT can imparts a negative surface charge on MWCNTs and a positive surface charge on TiO_2, thus unoxidized MWCNT plays as an electron transporter and significantly enhanced the photocatalytic activity of TiO_2.

2.10. Chemical vapor deposition (CVD)

Chemical vapor deposition (CVD) is a chemical process used to grow thin films. The substrate is exposed to one or more vaporized substances, and the vapor is thermally decomposed or reacted with other gases on the substrate surface to form thin film (Fig. 3). CVD is capable of producing CNTs thin films on various substrates. CNTs thin film can be grown on substrate by simultaneously providing organometallic and hydro carbon compounds in the method of CVD called spray pyrolysis. For the CVD process, catalysts are usually introduced in the growth process to promote the reaction. Ferrocene ($FeCp_2$) dissolved in benzene [48] and cyclohexane [49] are commonly used carbon resources.

CVD method is used for one-step deposition or multiple depositions. Different types of CVD have been employed to form different CNTs based composite film. Table 1 summarizes recent CNTs based composite thin film generated by CVD method or CVD combined with other fabrication techniques. The detailed parameters used are also presented.

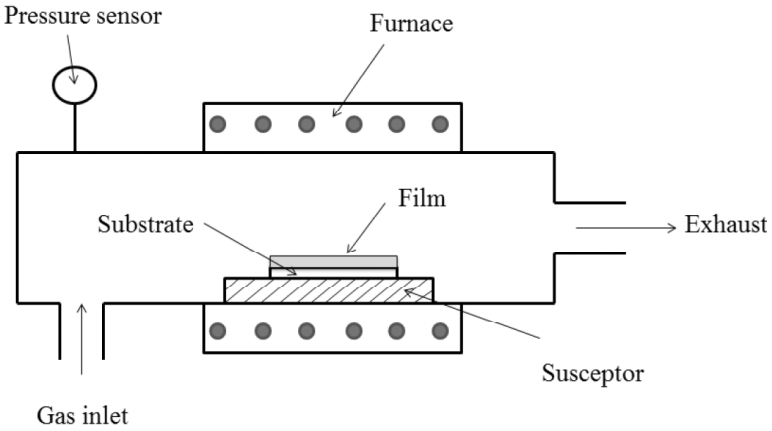

Fig. 3. Schematic diagram of typical thin film deposition using CVD method.

A simple CVD method for effective fabrication of N_2-encapsulated CNTs film by pyrolysis of $FeCp_2$ and acetonitrile (ACN) has been reported [50]. Batch-type pyrolysis of catalysts induced flow fluctuation of the reaction gases which lead to the growth of branched CNTs and rapid extrusion of N_2 along the conical catalyst particles, resulting in the encapsulation of N_2 inside the CNTs. Dong *et al.* [51] developed a one-step process of growing CNTs/graphene hybrid thin film onto copper foil (decorated with silicon nanoparticles) by a CVD method. A graphene film grows uniformly on the copper foil and CNTs exhibits bamboo-like multiple-wall structure sprout out from the Si NPs to form a network on top. However upon synthesis of CNTs based composite film, multiple depositions via CVD is another strategy for incorporating CNTs with other materials. CNTs/diamond thin film deposited on the stainless steels has been successfully synthesized by hot filament CVD (HFCVD) at 650 °C [52]. 1% and 5% CH_4/H_2 volume ratios are supplied for diamond and CNTs growth respectively. Similar method was also reported for the fabrication CNTs/Si thin film through two-step liquid injection CVD (LICVD) [53]. The first step involved in CNTs growth using liquid injection technique, wherein, m-xylene acts as the carbon source and $FeCp_2$ serves as the catalyst carried by argon and hydrogen at 770 °C. The second step

Table 1. Summary of recent CNTs based thin films prepared by CVD method.

Thin film type	Fabrication method	Carbon source	Catalyst	Operation temperature	Substrate	Reference
N_2-encapsulated CNTs	CVD	ACN	$FeCp_2$	850 ºC	Silica wafer	[50]
CNTs/Ni	rf PECVD	CH_4	-	650 ºC	Si/Si3N4	[88]
CNTs/Mo	CVD + electron-beam evaporation	Ethylene	Fe	720 ºC	Silicon	[108]
CNTs/((Ti,Al)N)	CVD + magnetron sputtering	Acetylene	Fe	700 ºC	Silica wafer/ high speed steel	[54]
CNTs/Graphene	CVD	Ethanol	-	800-900 ºC	Copper foil	[51]
CNTs/Diamond	HFCVD	CH_4	Stainless steels	650 ºC	Stainless steels	[52]
CNTs/GZO	ICPCVD + pulsed laser deposition	C_2H_2	Ni	700 ºC	Tungsten rod	[55]
SWCNTs/V_2O_5	CVD + hydrolytic deposition	$FeCp_2$	Sulphur + $FeCp_2$	1100 ºC	Aluminum foil	[124]
SWCNTs/MnO_2	CVD + Precipitation	$FeCp_2$	Sulphur + $FeCp_2$	1140 ºC	Copper foil	[125]
CNTs/Si	CVD	m-xylene	$FeCp_2$	770 ºC	Stainless steel	[53]

simply replaces hydrogen with silane gas, and adjusts temperature to 500 °C for growth of silicon.

Capable of producing highly dense and uniform CNTs films with excellent reproducibility and adhesion at relatively high deposition rate is one of the advantages of CVD. However, it also has limitations such as the difficulty to deposit multicomponent materials with well-controlled stoichiometry using multi-source precursors. To producing mechanically satisfying CNTs composite film, researchers put enormous efforts to investigate the combination of CVD with other deposition methods. For instance, CNTs embedded in ((Ti,Al)N) coated film was prepared combining in-situ CVD growth of CNTs with magnetron reactive sputtering deposition of a ceramic matrix ((Ti,Al)N) [54]. This combination joins the advantages between two deposition systems: CVD offers the possibility of tailoring the density, individual diameter, length and vertical alignment of CNTs, meanwhile magnetron sputtering offers unparalleled flexibility of thin films with a choice of well-defined stoichiometry and structure. Recently, Park and coworkers [55] prepared a CNTs and gallium-doped zinc oxide (GZO) thin film which combined inductively coupled plasma-CVD (ICPCVD) with pulsed laser deposition.

Formation of CNTs based thin films through CVD method is highly related to several parameters including the flow rate of the gaseous species, pressure of the chamber, temperature and catalyst. Huakang *et al.* [56] investigated the growth of CNTs on montmorillonite precursors treated with $Fe(NO_3)_3$ at 50 °C and 100 °C via CVD of acetylene. The results showed that CNTs embedded at 100 °C had narrower diameter distribution than that formed at 50 °C. The concentration of carbon in the precursor significantly affects the product yield because high carbon concentration causes catalyst deactivation. Thus, low carbon concentration in the gas phase is favored for production of CNTs thin films using CVD method. In addition, the catalyst density and growth time normally affect the density of the thin film. It is noted that CNTs films generated by CVD method may have the residual catalyst left which might influence the properties of devices. Importantly, CVD usually requires harsh conditions like high vacuum and high temperature process.

3. TECHNIQUES FOR CHARACTERIZATION OF CARBON NANOTUBE BASED THIN FILMS

As we described above, there are numerous methods for fabrication of CNTs based thin films, different materials and mechanisms involved in the processes to end up with thin films. It stands to reason that each type of thin films have different structure and properties. Characterization of CNTs based thin films not only measures the property of thin film which link to a specific application, but also is an acceptance test for the fabrication technique. Many characterization techniques have been developed for correlating the macroscopic manipulation with important properties of thin films at the micro or nanoscale. This section will be devoted to introduce the common experimental techniques for the characterization of CNTs based thin films.

3.1. Morphology analysis

For the composite thin films, there is a strong interrelationship between the structure and properties. The morphology and internal structure of the composite films is formed during the fabrication step. The CNTs represent in the thin film can be one of the entangled, agglomerated, uniformly dispersed or aligned states. Furthermore, different materials introduced into thin film can dramatically change its structure. The size, shape, and distribution of each component determined the film properties. Therefore, morphology observation is an essential part for thin film characterization. Scanning electron microscopy (SEM), transmission electron microscopy (TEM) and atomic force microscopy (AFM) are three common techniques used for analyzing thin film morphology.

SEM has already become a basic technique for visualizing the surface morphology of thin films. This method can intuitively distinguish the change between different films. Figs. 4a and 4b represent the one and six bilayer films of MWCNTs/gold nanoparticles (GNPs) [57]. The six bilayer film clearly displays higher coverage of MWCNTs and GNPs which indicates the successful growth of the multilayer assembly. Additionally, the difference between the neat and composite film can also be determined by SEM. Figs. 4c and 4d show the images of annealed TiO_2 and MWCNTs/TiO_2 film taken by the field emission-SEM [58]. Both images display a similar surface structure of TiO_2 with coarse grains of approximately 1 μm in size. The MWCNTs aggregations present at Fig. 4d, suggests that the MWCNTs/TiO_2 hybrid film is successfully formed and the incorporation of MWCNTs does not significantly alter the surface area of TiO_2.

TEM is a powerful imaging technique to characterize atomic features found in nanostructures. TEM usually provides more detailed structural infomation

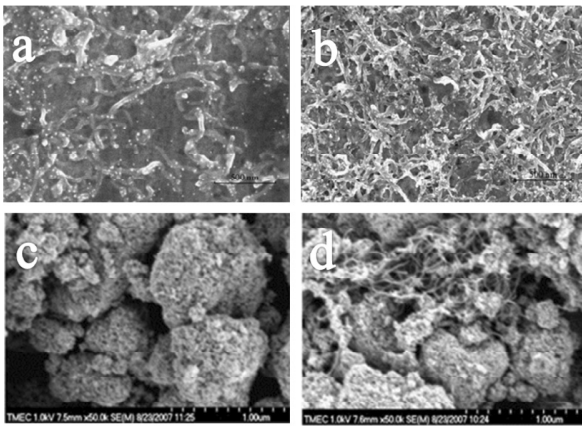

Fig. 4. SEM images of (a) 1 bilayer MWCNTs/GNPs thin film. (b) 6 bilayers MWCNTs/GNPs thin film. (c) Pure TiO2 thin film. (d) MWCNTs/TiO2 thin film. Reprinted from Ref. [57,58], Copyright 2013 with permission from Elsevier.

than SEM because it is capable of achieving a point-to-point resolution down to 0.1 nm. TEM imaging is particularly important in studying the relationship between CNTs and composited nanoparticles. Fig. 5a illustrates the TEM image of SWCNTs/Ni(NiO) composite deposited onto the cathode by the electro-deposition method [59]. Compared with the inset image of pure SWCNT, it clearly showed that the bundle of SWCNT were decorated uniformly with nanoparticles of 2-7 nm. Furthermore, two types of interaction modes between Ni and SWCNTs were found: one was Ni located on the fringe of SWCNTs bundles, where the diameter of SWCNTs was about 1-2 nm and the size of Ni particles was around 5-10 nm, another one was Ni particles insert the space of thin SWCNTs bundles. In terms of CNTs/poly-electrolytes composite thin film, TEM plays important role in investigating the change of film structure, which is usually hard to be confirmed by SEM. Figs. 5b and 5c are the TEM images of oxidized MWCNTs and MWCNTs/poly(N,Ndiethylacrylamide) (PDEAAm) composite respectively [60]. It is obvious that the diameter of MWCNT/PDEAAm composite is much thicker than the oxidized MWCNTs. The surface of oxidized MWCNTs is smooth and clear, while the MWCNTs/PDEAAm composite has fuzzy and translucent edges. Those differences prove that a layer of PDEAAm was wrapped on the surface of MWCNTs. The widespread use of AFM for characterizing thin film sample is attributed to the accurate threedimensional reconstruction of the

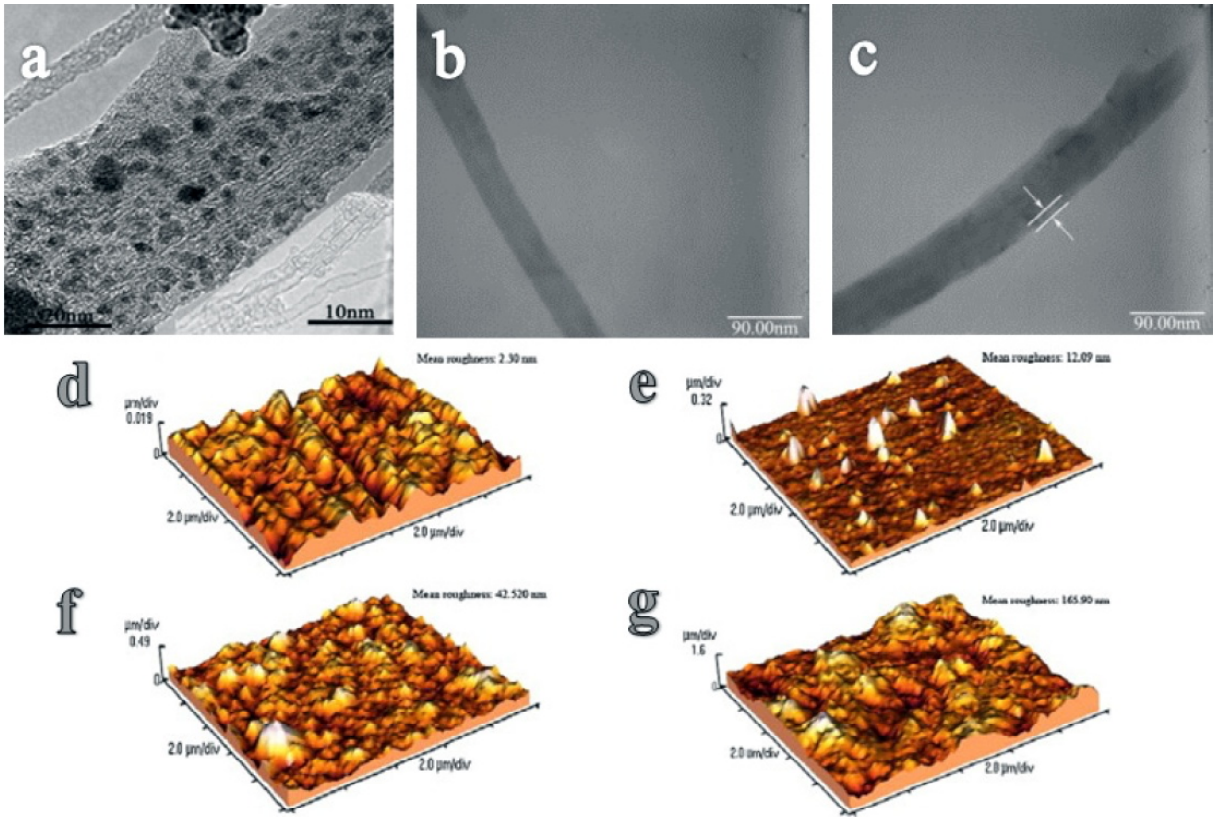

Fig. 5. TEM images of (a) SWCNTs/Ni(NiO) composite. (b) Oxidized MWCNTs. (c) MWCNTs/PDEAAm composite. AFM images of (d) GCE. (e) GC/CoPc. (f) SWCNTs/GC (g) SWCNTs/GC + CoPc. Reprinted from Ref. [59,60,61], Copyright 2013 with permission from Elsevier.

sample topography with atomic resolution. AFM also allows imaging of the surface roughness of the sample. Figs. 5d-5g show the AFM images of bare glass carbon electrode (GCE) (d), cobalt phthalocyanine (GC/CoPc) (e), SWCNTs/GC (f) and SWCNTs/GC + CoPc (g). There are clear differences in terms of surface roughness values are collected, which confirming the different compositions exist in the hybrid thin films. Fig. 5e gives island-like structure which indicates the CoPc cluster adsorbed on GC electrode. Conversely, SWCNTs observed from Fig. 5f are randomly distributed but completely covered the GC electrode surface, when comparing to unmodified GC electrode (Fig. 5d). In the case of SWCNTs/CoPc/GC electrode, CoPc is distributed with a non-uniform island-like structure. On the other hand, the electrical properties of CNTs based thin film could also be measured by AFM. The electrical properties of single MWCNT from a macroscopic composite thin film of aligned MWCNTs embedded in polymer matrix was studied by Villeneuve *et al.* [61] It is the first presentation of the conduction profile of a single vertical CNT. Results also indicate only the external sheets are conductive.

3.2. Spectroscopic characterization

Spectroscopic analysis techniques are powerful methods for characterizing many aspects of CNTs based thin films, such as the amount of material loading during the fabrication process, the chemical composition in the surface region, elemental composition of thin film, and the identification of CNTs modification. There are four common spectroscopic analysis techniques for characterizing CNTs based thin film: Raman spectroscopy, Fourier-transform infrared spectroscopy (FTIR), ultraviolet-visible (UVVis) spectroscopy and X-ray photoelectron spectroscopy (XPS).

Raman spectroscopy is a technique used to study the vibrational, rotational, and other low frequency modes of a material. It relies on the inelastic scattering, also called Raman scattering of monochromatic light. In Raman scattering, the difference in energy between the absorbed and reemitted photons corresponds to the energy required to excite a molecule to a higher vibrational energy band. All allotropic forms of carbon are active in Raman spectroscopy. However, the position, width, and relative intensity of absorption bands are different according to the different forms of carbon. The typical Raman spectroscopy of CNTs are shown in Fig. 6a [62]. The characteristic features of CNT including the radial breathing mode (RBM), the D band, G band, G' band and the second order modes are clearly seen. When CNTs are incorporated into thin films, these characteristic peaks will change which gives the information on the structural change. The absorption intensity and band change have also been observed for functionalized CNTs. Yim *et al*. [20] reported the upword shift of G' band, which is interpreted as a signature of CNTs film compression following water evaporation during nitric acid treatment. Wang *et al.* [46] also reported the small shift of G-band of MWCNTs after isophthalic acid treatment. Besides, a lower in the intensity ratio of D band (ID) to G band (IG) implies a better graphite structure and a higher degree of graphitization. Additionally, the reduced intensity of G-band in Raman spectra can be detected when CNTs based gas sensor after exposing to target gases [63].

FTIR is another widely used spectral technique for characterization of CNTs based thin films. FTIR is often used to confirm the surface modification of CNTs and reveals the chemical structure of the compounds that attached on CNTs. It sometimes also gives extra information on the property change of materials. For example, Fig. 6b shows the FTIR spectra of polyaniline (PANI), MWCNTs, and MWCNTs/PANI composite [64]. Compared with PANI, the spectrum of MWCNTs/PANI composite has no new absorption peak occurring, but the changes in peak shape and absorption intensity were observed. Specifically, the peaks at 1205, 1105, 847, and 1318 cm^{-1} became wider and stronger. There changes are due to the spectra overlapping and the interaction between MWCNTs and PANI which gives the evidence that PANI is attached to the MWCNTs. In addition, the peak at 1105 cm^{-1} is a measure of the degree of delocalization of electrons, which is related to the characteristic of the conductivity of PANI [65, 66]. The MWCNTs/ PANI composite has a stronger absorption at 1105 cm^{-1} than pure PANI, which implies that the PANI's conductivity is improved when attached to MWCNT.

UV-Vis spectroscopy is a quantitative measurement of the reflection or transmission properties of a material as a function of wavelength. This absorption spectroscopic technique is very useful in monitoring the growth of CNTs based thin film. Fig. 6c demonstrates the use of UV-Vis spectroscopy to study the LbL self-assembly of MWCNTs/PDDA multilayers thin film. The spectra clearly showed a regular absorbance increase along with the number of PDDA/MWCNT bilayers which confirmed the stepwise formation of MWCNTs/PDDA multilayer film [37]. In addition, the absorbance data gives the information on how much of the materials were de-

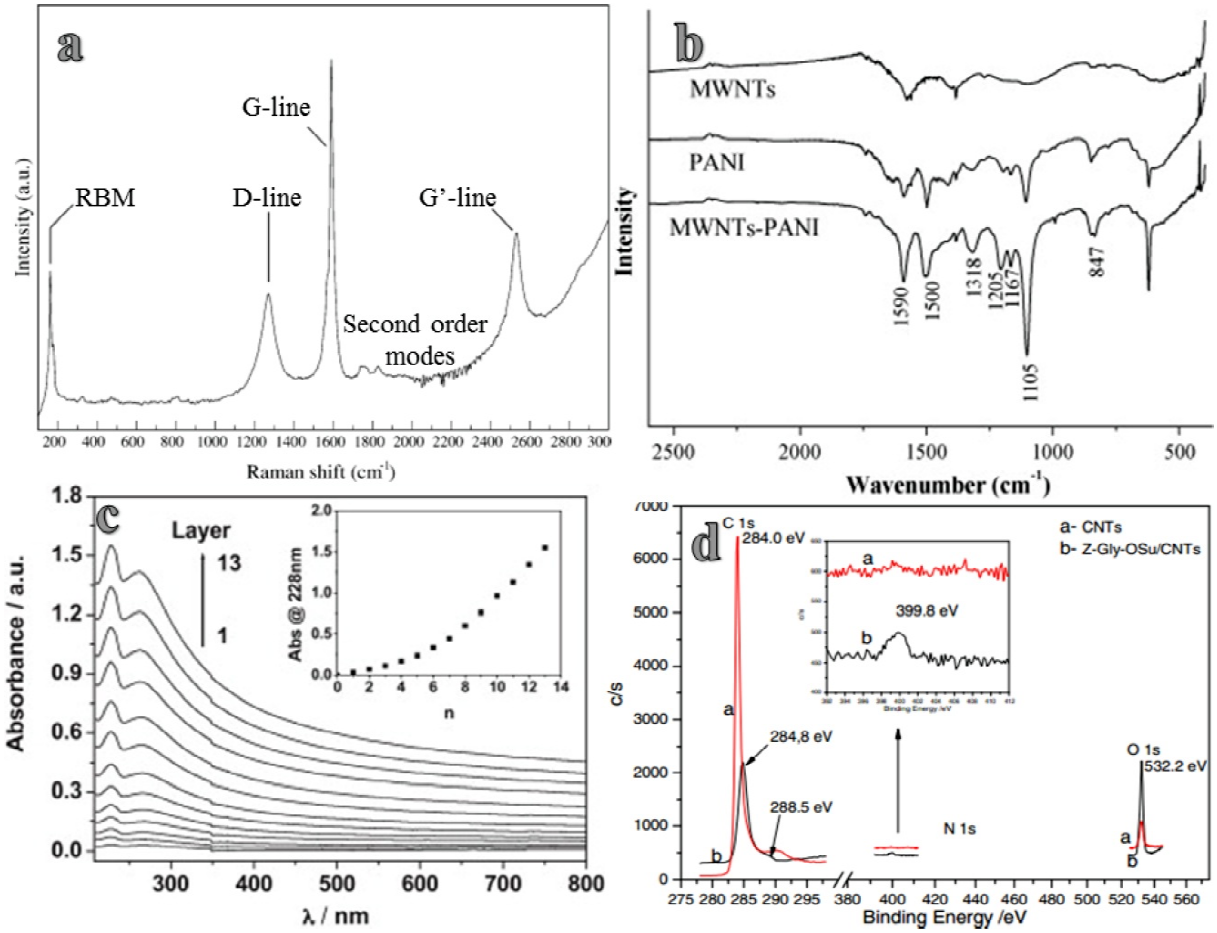

Fig. 6. (a) Raman spectrum of CNT showing its most characteristic features of radial breathing mode (RBM), the D band, G band, G' band, and the second order modes. (b) FTIR spectra of MWCNT, PANI, and MWCNT/PANI composite. (c) UV-vis absorption spectra of PEI/PSS(PDDA/MWCNTs)n (*n* = 1-13) multilayer films on quartz slide. The inset shows the absorbance maximum at 228 nm as a function of bilayer numbers. (d) XPS spectra (C_{1s}, N_{1s}, and O_{1s}) of pristine CNT and Z-Gly-OSu-functionalized CNT. The inset figure is the magnified N1s spectra. Reprinted from Ref. [62,64,67,68], Copyright 2013 with permission from Elsevier.

posited during the assembly process. The inset of Fig. 6c represents the absorbance at 228 nm as a function of bilayer numbers, indicating that the initial growth of the film is slow then it becomes much faster from the 6th layer with more than double amount of the materials being adsorbed in each deposition cycle. Similar to FTIR, the peak appearance and shape change of UV-Vis spectra is an alternative way to determine the compounds that added to the CNT [67].

Finally, XPS is a powerful surface analytical technique being capable of collecting the information of a surface layer (2-5 nm depth), such as composition, chemical states and quantity of an element. XPS has been successfully used for characterizing a variety of thin films. Wei and coworkers [68] used XPS to identify the functionalization of CNTs with Z-glycine Nsuccinimidyl ester (Z-Gly-OSu). Fig. 6d shows the XPS spectra of pristine CNTs and the Z-Gly-OSu- functionalized CNTs at the peaks of C_{1s}, N_{1s}, and O_{1s}. The binding energy of C_{1s} peak of pristine CNTs is located at 284.0 eV. After functionalization, two C_{1s} peaks have been found in spectrum. The original peak showed little shift to 284.8 eV, additional peak appeared at 288.5 eV, may respond by N-C=O from the amide bond. N_{1s} spectra also improved the functionalization happens at CNT because there is no peak appear at pristine CNTs, but one new peak at 399.8 eV has been found in Z-Gly-OSu-functionalized CNTs sample, which can be ascribed to the N atoms of Z-Gly-OSu linker.

3.3. Thermal analysis

The thermal stability of the lms is experimentally determined by the threshold temperature during

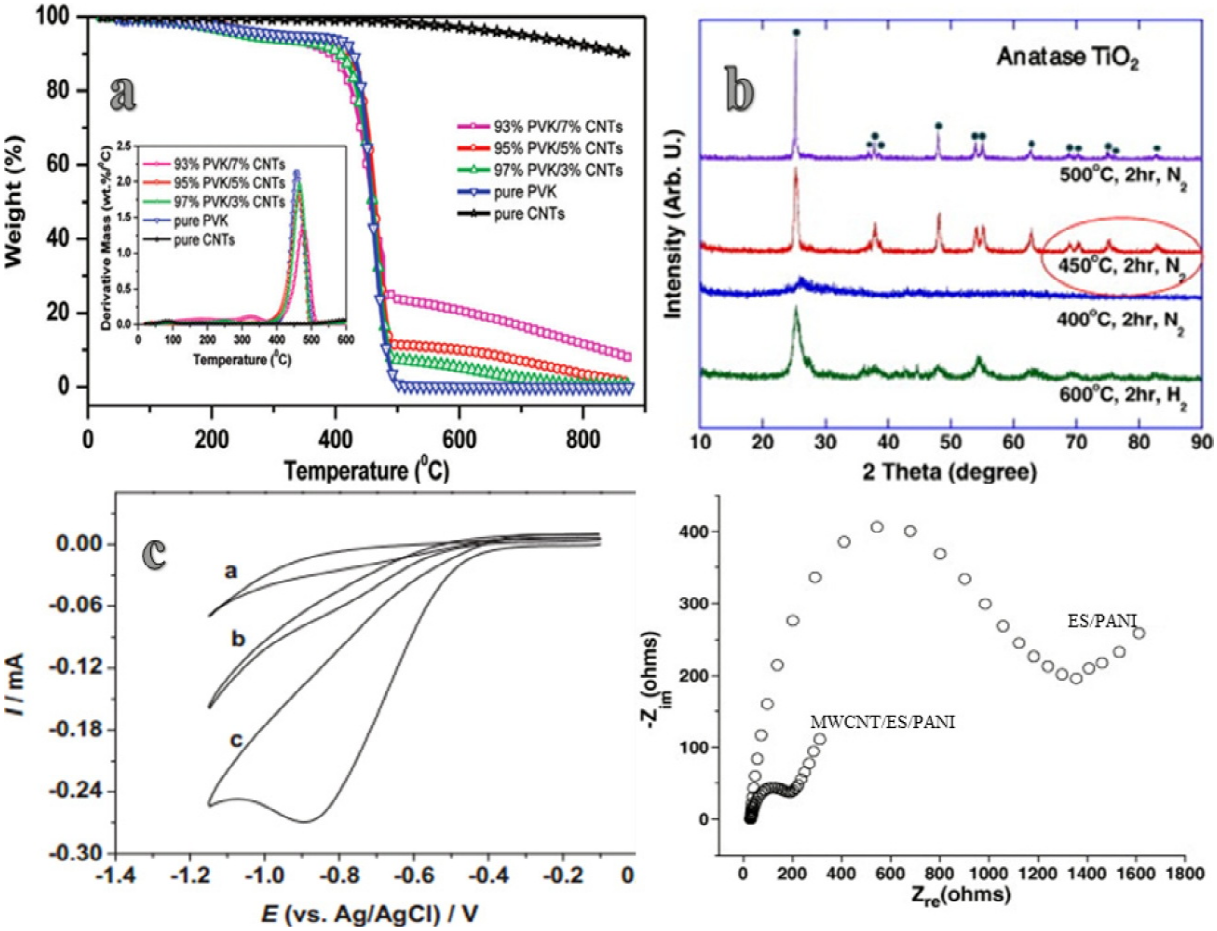

Fig. 7. (a) TGA thermograms of pure MWNT, pure PVK, and PVK/MWNT under N_2 at a heating rate of 20 C/min. Inset Graph of DTG curves of pure MWNT, pure PVK, and MWNTs/PVK nanocomposite solutions. (b) XRD pattern of heat-treated CNTs-TiO_2 hybrid thin film under various temperatures. (c) The voltammetric response to 1 mM hydrogen peroxide at bare ITO electrode, [PEI/PSS/$(PDDA/MWCNT)_6$] and [PEI/PSS/$(PDDA/MWCNTs)_6$/Ag NPs] modified ITO electrodes in pH 7.0 PB solution. Scan rate: 50 mV/s. (d) Impedance spectra of electrophoretic deposited ES/PANI and MWCNTs/ES/PANI composite film. Reprinted from Ref. [37,69,74,77], Copyright 2012 with permission from Elsevier.

annealing at which the lm structure begins to change and roughen. Some applications of CNTs based thin films require working at high temperature condition, so the thermal limitation is an important feature of the film. Thermal gravimetric analysis (TGA) and derivative thermal gravimetric (DTG) methods are usually used for testing the thermal stability of CNTs based thin film. TGA is based on the measurement of mass loss of material as a function of temperature. A DTG presents the rate of mass change (dm/dt) as a function of temperature. Both data are obtained when a substance is heated at a uniform rate or kept at constant temperature.

The thermal characterization has found that the adding CNTs could improve the thermal stability of polymer composite. Fig. 7a shows typical TGA thermograms, which depict the mass losses of MWCNTs, poly (N-vinyl carbazole) (PVK) film and different ratios of the MWCNTs/PVK composite film upon heating in a nitrogen atmosphere [69]. It is clear seen in the graph that the pure MWCNTs exhibited a high stability showing only a 2% weight loss after heating to 500 °C. PVK represented lower stability which starts degradation at 260 °C. Comparing MWCNTs/PVK composite films with different ratios of MWCNTs, it was observed that the increasing percentage of MWCNTs led to less weight loss, suggesting that the MWCNTs improved the thermal stability of the composite film. The reason of this improvement can be explained in two aspects. Polymer chains near the nanotubes may degrade more slowly, which helps to increase the decomposition temperature [70]. Another reason may be due to the higher thermal conductivity of MWNTs that facilitates heat dissipation within the composite.

The DTG curves can provide information about the point where significant weight loss occurs. From the DTG curves (Fig. 7a insert), it is clearly seen that there is a shift to higher degradation temperature for the MWNTs/PVK composite as compared with the pure PVK. To accurately identify the degradation components and their thermal properties, dynamic rate control method of TGA has been widely used. Li *et al.* [71] employed TGA to analyze the CNTs/TiO_2 composite synthesized by variety precursors. The results showed the composites synthesized bydifferent precursors have quite different thermal properties, which should be attributed to different morphology, compactness and crystallinity of TiO_2 coatings as a function of precursor type.

3.4. X-ray powder diffraction (XRD)

XRD is the most popular X-ray scattering technique for characterizing the crystallographic structure of samples. The X-ray diffraction pattern of the CNTs sample usually presence of two peaks at $2\theta = 26°$ and 43° corresponding to the 002 and 100 reflection of the carbon atoms. The functionalization process will narrow those peaks due to the loss of amorphous carbon [72]. XRD is also capable of studying the mean tube diameter, the finite size of the bundles and the diameter dispersity of CNTs. In terms of CNT based composites, XRD patterns reveals the CNTs/copolymer composite has a more crystalline nature than the bare copolymer [73]. Identification of the crystal phase in certain CNTs based thin film is crucial, such as CNTs/TiO_2 thin film as the crystal phase of TiO_2 is highly related to its photocatalytic activity. Anatase has the best photocatalytic rate in several TiO_2 crystal phase because of its larger band gap energy between valence band and conduction band. The amorphous TiO_2 can be transformed into anatase or rutile structure according to the heating temperature. Fig. 7b exhibited XRD pattern of heat-treated CNTs-TiO_2 hybrid thin film under various temperatures, which attest amorphous TiO2 was well crystallized eventually into anatase phase at 450 °C [74].

3.5. Electrochemical characterization

CNTs based thin films offer potential applications as conducting or semiconducting layers in various types of electronic, optoelectronic, and sensor systems. Cyclic voltammetry (CV) is the most widely used technique for investigating the electrochemical property of CNTs based films, which is performed by cycling the potential of a working electrode and measuring the resulting current. Our group studied the electrocatalytic activity of MWCNTs/Ag NPs composite film toward hydrogen peroxide by using the CV technique [37]. Three-electrode system has been used in measurement, including a film modified ITO electrode as the working electrode, a platinum disk as the auxiliary electrode and an Ag/AgCl wire as the reference electrode. Fig. 7c demonstrates the electrochemical responses of 1.0 mM H_2O_2 at bare ITO, $(MWCNT/PDDA)_6$ and $(MWCNT/PDDA)_6$/Ag NPs deposited electrodes. We found the redox activity of H_2O_2 could be enhanced by MWCNT and further improved in the presence of Ag NPs. Beyond that, CV is also used to evaluate the assemble process of multilayer films. The regular change of both the anodic and cathodic peak current is an evidence for alternative layers formed on electrodes.

Electrochemical impedance spectroscopy (EIS) usually provides detailed information on the impedance change of the electrode interface. As a steady state technique with small potential variation, EIS is more reliable than CV for measuring the capacitance with minimized effect from noncapacitive Faradaic contributions [75]. In a typical impedance spectrum, a semi-circle part at higher frequency range and a straight line part at lower frequency range are included in the Nyquist plot. The diameter of the semi-circle at higher frequency range in the Nyquist plot equals to the electron transfer resistance [76]. The dependence of impedance spectra of the CNTs/conducting polymer composite is considered for studying the characteristics of lm structures, kinetics, and mechanisms of charge transfer and ion transport in the CNTs/polymer lm interface. As an example, Fig. 7d shows the impedance spectrum of the electrophoretic deposited emeraldine salt (ES)/PANI and MWCNTs/ES/PANI composite film [77]. The remarkable decrease in the diameter of the semicircle (indicative of charge transfer resistance) was detected in the composite film. The smaller semicircle indicates that the charge transfer resistance for MWCNTs/ES composite film is much lower than the ES film. Besides this, the presence of MWCNTs could also serve as 'conducting bridges' between ES and electrode surface.

4. APPLICATIONS

4.1. Sensors

The hollow structure of CNT contributes to a large surface area and volume ratio, which makes it appropriate for physisorption and chemisorption of sensing targets. Various types of thin film sensors have been fabricated and investigated based on

SWCNTs, double-walled carbon nanotubes (DWCNTs) and MWCNTs.

4.1.1. Temperature and humidity sensors

Humidity can influence several properties of CNTs including electrical conductivity, electrical transport property and impedance. There is a relationship between the humidity and the capacitance of a CNTs film sensor: the capacitance of sensor increases or resistance decreases with increasing humidity level [78,79]. Highly sensitive humidity sensor has been achieved by fabricating CNTs/PDDA composite films on to Si/SiO_2 substrate through LbL self-assembly technique [80]. The resistance of sensor responds to humidity from 20% to 98% shows exponentially increasing after annealing treatment. The response time of the sensor is around 8 s, and the recovery time only in 35 s. Poly(ethyleneimine) (PEI) and MWCNTs composite films sensor reported by Yu *et al*. [81] is capable to respond humidity level even cross 5-97%, the response and recovery time are 2 s and 30 s respectively.

It is generally known that suitable acid treatment is a common method to enhance the solubility of CNTs and forming functional groups to the sidewalls, like -COOH. The incorporation of functionalized CNTs with cationic polyelectrolytes into the multilayer films through LbL self-assembly can form high sensitive humidity sensor. The comparison shows the sensitivity of SWCNTs-COOH/PDDA thin film sensor is more than 20% higher than SWCNTs/PDDA thin film sensor [82]. This phenomenon may be caused by the high contents of π-π* transition structures exist in SWCNTs-COOH/PDDA thin film which could help adsorb more water molecules.

Many mechanical, medical, chemical, agricultural, and food industries extensively use temperature sensors. CNTs based sensor has been created ground on the conductance change response to the temperature. The electrical transport of highly disordered MWCNTs of large outer diameter (~60 nm) has been found to be dependent on temperature change [83]. As the temperature elevate, the conductivity of CNTs increases accordingly. This conduction mechanism can be explained by the Percolation theory [84]. The CNTs based thin film sensor can be assumed as a bulk hetero system, CNTs layers are highly sensitive to the change of temperature which result by the increasing of interparticles contact areas and intrinsic conductivity of the nanoparticles take place as rising temperature. For the purpose of using CNTs based sensors in air and water under normal living conditions for applications, Naoki Inomata and Fumihito Arai [85] investigated the temperature coefficients of resistance of single CNT in water, air and vacuum, which are $0.735x10^{-3}$, $0.422 x10^{-3}$, and $0.214 x10^{-3}$/°C, respectively. Temperature sensor fabricated by the sequential deposition of thin layers of glue and CNTs nanopowder on a paper substrate reveals that there is average 10-20% decrease in DC resistance of the sensors during the temperature increase from 20 to 75 °C [86]. Not only that, CNTs based thin film sensor also shows great performance at low temperature. Saraiya *et al.* [87] reported the preparation of CNTs film on the nickel deposited float glass substrate by the ion beam deposition technique. The resulting film had more than 600% change in resistance when the temperature change from 300K to 10K.

4.1.2. Gas sensors

The unique chirality of CNTs contributes to the p-type semiconducting property. The conductivity of CNTs will change significantly when gas molecules are absorbed [88,89]. CNTs based sensor outperform conventional sensors in terms of large adsorptive capacity, highly sensitive to small quantities of gases at room temperature and quick response time. Because the physisorption and chemisorption synergistic effect properties that cause the response time of CNTs based sensors are varying for different target gases [90]. For the purpose of enhancing the sensitivity and selectivity, CNTs is often hybrid with other materials. CNTs mixed with silane shows the ability to enhance the selectivity of certain gases and also improve the mechanical adhesion to the substrate [91]. In terms of enhancing sensor sensitivity, other sensing materials such as metal oxide semiconductors are usually chose for incorporation. A MWCNTs-doped SnO_2 thin film gas sensor was reported by Wei *et al.* [92] which showed much higher sensitivity than the pure SnO_2 film sensor. The performance of the MWCNTs-doped SnO_2 sensor was based on the change in the barrier height and the conductivity of the MWCNTs/SnO_2 sensitive layer. When NO_2 is absorbed, the depletion layer at the p-n junction is modulated. It leads to the fact that this type of gas sensor is capable to response to low concentrations of NO_2 down to the ppb range. Synthesis of CNTs-conducting polymer composites sensor also tailor the electronic and mechanical properties based on morphological modification or electronic interaction between the two components. For example, a gas sensor based on CNTs/

Table 2. Summary of the sensing properties of various CNT based thin film gas sensors.

Sensor description	Target species	Detection level/range	Operation temperature	Response time	Recovery time	Reference
MWCNTs-doped TiO_2 xerogel	CO	50 ppm	300 °C	4 s	16 s	[26]
MWCNTs-Al_2O_3	NH_3	6-25 ppm	RT*	10 min	20 min	[27]
SnO_2-arc-discharge	NH_3	1 ppm/NH_3	RT*	-	-	[63]
SWCNTs	O_3	20 ppb/ O_3				
Horizontally aligned CNTs	H_2	200-16,000 ppm	RT*	8-17 min	2.4-4.5 min	[126]
N-doped SWCNTs	NO_2	200 ppb	150 °C	25 min	30 min	[127]
Pd-decorated MWCNTs	H_2	350 ppm	RT*	150 s	210 s	[128]
CNTs/reduced graphene	NO_2	0.5-10 ppm	RT*	-	-	[129]
Polyaniline-MWCNTs	NO_2	100 ppm	RT*	5 min	10 min	[130]
Acid modified MWCNTs	SF_6	0.5-20 ppm	RT*	-	-	[131]
WO_3/MWCNTs	NO_2	5 ppm	RT*	12 min	15 min	[132]
ZnO/SWCNTs	NO_2	1-1000 ppm	25-300 °C	5 min	8 min	[133]

poly(oanisidine) (POAS) composite offers a sensitivity of approximate 28% compared to a mere 4% by CNTs alone for the detection of HCl vapor [93]. This extended detection capability is attributed to the direct charge transfer with electron hopping effects on intertube conductivity through physically adsorbed POAS between CNTs.

Stability in different environment is always a crucial aspect for gas sensors. Ceramic materials has been involved to reinforce the impart stiffness, strength, and toughness of CNTs due to its excellent mechanical properties and relatively low density. Depositing CNTs films onto TLM platform can improve the temperature stability of the sensor due to the top layer of platinum.

The major drawback of the gas sensors is its slow and incomplete recovery. Some literature depicted the recovery time of the senor was approximately 10 h [94]. Researchers have put lots of effort to surmount this issue. Valentini *et al.* [95] have demonstrated that heat treatment at 465-500K could significantly reduce the recovery time to 1 h. On the other hand, UV treatment could also reduce the recovery time by evicting the absorbed molecules out of the sensor. Except of using external forces, combining CNTs to certain materials can also shorten the recovery time conspicuously. Table 2 summarizes the sensing properties of some recent reported CNTs based film gas sensors.

4.1.3. Biosensors

Basically, the improvement of biosensor performance requires a good signal transducer material which in charge of the communication between the target biomolecule and the sensor surface. The unique physical and chemical properties of nanostructured CNTs based thin film have paved the way to achieve advanced electrochemical biosensors. For example, CNTs could serve as electric conductor and electrode modifier in pasty electrodes and oxidase based biosensors. Patolsky *et al.* [96] reported the first study on the aligned reconstitution of a redox glucose oxidase (GO_x) on the CNTs modified electrode surface. SWCNTs act as nano-connectors between the active site of the enzyme and the electrode. According to the surface coverage of the GO_x-CNT units, the turnover rate of electron transferred to the electrode is about 4100 s^{-1}, which is sixfold higher than the active site of GO_x to its natural O_2 electron acceptor. The experiment also showed that the electron transmission velocity was depended on the length of SWCNT. In addition, the CNTs thin film architectures have been studied to develop high sensitive and selective immunosensor. Ou *et al*. [97] reported the use of MWCNTs/GNPs/thionine film as a label-free amperometric immunosensor for carcinoembryonic antigen (CEA) detection. The MWCNTs act as a support to the redox mediator thionine as well as the conductor to enhance the electron transfer of the mediator to the electrode. The results showed the immunosensor was highly sensitive to CEA with a detection limit of 0.01 ng mL^{-1} and it could be regenerated 10 times by simply immersing the immunosensor in a stirred 5 M urea solution for 5 min and washing with water.

One challenge in biosensor development is that the immobilized biomolecules easily denature lead-

ing to the loss of their bioactivity. LbL selfassembly technique was found to be able to improve this issue. A DNA biosensor has been fabricated based on the LbL covalent assembly of GNPs and MWCNTs-CONH-$(CH_2)_2$-SH on the Au electrode which showed the great stability and reproducibility to detect singlebase mismatched DNA sequence [57]. A LbL self-assembly technique combined with MWCNTs modification was reported for fabricating choline sensors [98]. This choline sensor showed a linear response in the concentration range between $5x10^{-7}$ and $1x10^{-4}$ M and a detection limit of $2x10^{-7}$ M. Except for quick response time, six amperometric measurements for 0.1 mM choline suggest that the sensor with MWCNTs has lower relative standard deviation than the sensor without MWCNTs. The long-term storage stability experiments showed the choline sensor without MWCNTs retained 78.5% of the initial sensitivity after 1 month while the sensor include MWCNTs retained 89.5%.

4.2. Energy conversion and storage

Solar energy has a great potential as a green energy owing to its abundance and even distribution in nature. Thin film based solar cells has attracted large interest because of their low fabrication cost and high energy conversion performance. Studies have showed that incorporating CNTs into solar cells can significantly improve the photo-conversion efficiency. For example, incorporating MWCNTs into the TiO_2 active layer contributes to an outstanding improvement in the energy conversion efficiency of dye-sensitized solar cells (DSSCs) [58]. This improvement attributes to the capacity of CNTs to facilitate the charge transport across the photoactive layer resulting in a reduced rate of charge recombination [99]. CNTs based thin film solar cells potentially offer many advantages beyond the traditional DSSCs. As the semiconducting property of CNTs for photo conversion, solar cells do not need to rely on dyes [100]. Moreover, Pt is commonly used as counter electrode in solar cells which represent an undesirable reliance on noble metals that may restrict for large scale devices. Another problem with Pt is the degradation due to contact with electrolyte [101]. In contrast, the chemical inert of CNTs let it become a great candidate as counter electrodes [102,103]. Furthermore, the conducting coating is not required for solar cells since CNTs based thin film itself is a transparent conductor which banishing the need of In coating.

Fuel cells are promising choice for clean energy due to its eco-friendly system, high energy conversion efficiency, high power density, and low operating temperature. Recent research revealed that the CNTs can greatly improve the performance of fuel cells by offering a high surface area support to the Pt nanoparticle catalyst. The use of CNTs also improves the dispersity of Pt nanoparticles, promotes electron transfer and enhances stability. Girishkumar and co-workers [104] demonstrated that compared with commercial Pt/carbon black catalyst, SWCNTs/Pt film electrodes exhibit a lower onset potential and a higher electron-transfer rate constant for oxygen reduction. The accelerated durability test was carried out in $HClO_4$ solution which showed electrochemically active surface area of Pt/carbon black has continuously decrease during the test and finally bellow to SWCNT/Pt after 36 h, even though the Pt/carbon black has a higher electrochemically activity surface area than SWCNTs/Pt before the durability test. The result indicates the SWCNTs could enhance the stability of the electrocatalyst for long-term use. However, the scarcity of durability test is carried out in acidic solution which cannot fully confirm the performance in actual environment.

Biofuel cells provide new opportunities for the sustainable production of energy from biodegradable compounds which could serve as power sources for implanted devices like pacemakers, sensors, and drug dispensers. The properties of CNTs can be used for increasing effective surface area of electrode, and at same time for the construction of extended conducting networks. Fig. 8a shows the schematic of anthracene and anthraquinone covalently modied SWCNTs as cathodes for biocatalytic reduction of dioxygen [105]. The outcome reveals that glassy carbon electrode covered with arylated SWCNTs and coated with a layer of Nafion containing laccase was a very efficient cathode in hybrid battery. More than 2 Mw/cm^2 power densities and 1.5 V open circuit potential was obtained in the experiment that Zn wire was used as anode. Fig. 8b briefly illustrates the construction of an enzymatic fuel cell based on CNTs [106]. The small diameter of CNT allows a close approach to the redox active site of redox enzyme for electronic communication, therefore regenerate the biocatalysts during direct electron transfer or act as redox mediators to help electron transfer. For instance, fuel cell that has glucose/O_2 biofuel cell with $(MWNTs/thionine/Au\ NPs)_8$ GDH film modified ITO electrode as anode and the (MWNTs/PLL/laccase)15 lm modied ITO electrode as a cathode showed 700 mV open-circuit voltage and 329 mW/cm^2 power density at 470 μV of the cell voltage [107].

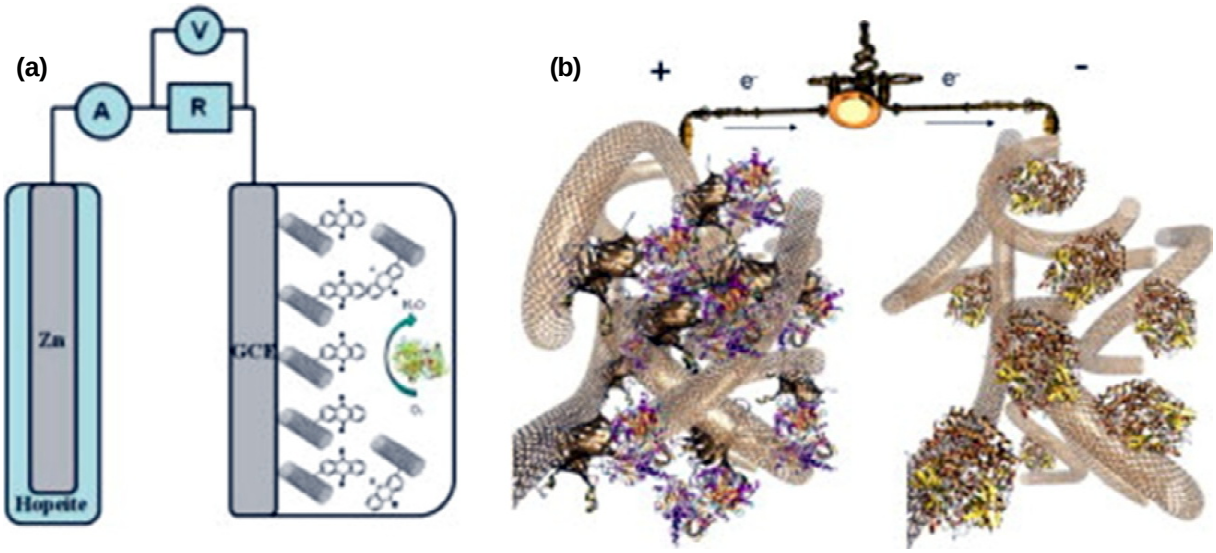

Fig. 8. Schematic representation of (a) biobattery circuit and (b) enzymatic fuel cell based on CNT. Reprinted from Ref. [105,106], Copyright 2013 with permission from Elsevier.

CNTs based electrodes have previously been shown to have excellent properties in supercapacitor applications. For example, the CNTs film with intrinsic bottom metal contacts to construct mechanically bendable, densely aligned CNTs forests was used for supercapacitor which possesses salient features include simple fabrication process, great transfer of charge from the aligned CNTs to the substrate and easy integration with a variety of surfaces and morphologies. Kozinda *et al.* [108] reported a CNTs forest of 5x10 mm^2 in area on Au/Kapton® film showed a specific capacitance of 7.0 mF/cm^2. Besides, CNTs also plays important roles in hybrid supercapacitors which combine the electrical double layer capacitive electrode and the pseudo-capacitive electrode. Electrochemical conducting polymers and metal oxides are usually deposited onto CNTs to increase the total capacitance through faradaic pseudo-capacitance effects. Zhang *et al.* [109] demonstrated that the MWCNTs/PANI composite film electrode showed better capacitive characteristics than the pure PANI electrode. The test obtained specific capacitance of 500 Fg^{-1} by composited film even if the content of MWCNTs is only 0.8 wt.%. On account of the presence of MWCNTs, the composite films possess more active surface area for faradaic reaction, larger SC, as well as having lower resistance and better cyclic stability.

4.3. Photocatalytic applications

Incorporating CNTs thin films with certain photocatalysts, especially TiO_2 is currently being considered for many applications including degradation of environmental pollutants in aqueous contamination, wastewater treatment, and air purification. There are two mechanisms being discussed to explain the CNTs-enhanced photocatalytic activity of TiO_2. The first mechanism was proposed by Hoffmann *et al.* [110]. A highenergy photon excites an electron from valence band to the conduction band of anatase. Photogenerated electrons formed in the space-charge regions are transferred into the CNTs and holes remain on the TiO_2 to take part in redox reaction. Another mechanism reported by Wang *et al.* [25] is based on the premise that CNTs may enhance TiO_2 photocatalytic activity by acting as a photosensitizer. The photogenerated electron is injected into the CB of TiO_2, simultaneously a positive charged hole formed by electron migrating from TiO_2 valence band to CNTs and reduction of the so formed hole by absorbed OH-oxidation.

CNTs/TiO_2 composite films have been tested for the photodegradation of various chemicals such as Porcion Red [111], phenol [25] and methylene blue [71]. All these studies have revealed that the addition of CNTs could enhance the photocatalytic efficiency of TiO_2. Tettey and co-worker [111] test the photocatalytic activity of MWCNTs/TiO_2 composite thin film and pure TiO_2 thin film by degradation of Porcion Red under UV irradiation. The photodegradation results showed that the incorporation of MWCNTs leads to an approximately 2-fold increase in the first order rate constant of photocatalytic activity of TiO_2. Additionally, the potential application of antibacterial of CNT/TiO_2 thin film has been recently studied. Akhavan *et al.* [112] investigated visible light photoinactivation of Escherichia

coli bacteria on the surface of CNTs-doped TiO_2 thin lms with various CNTs contents. The antibacterial activity of the nanocomposite thin lms in the dark was enhanced by increasing the CNTs content which assigned to the partial bactericidal activity of MWCNTs themselves. By increasing the CNTs content from 0 to 40 wt.% and annealed at 450 °C, the effective band gap energy decreased from 3.3 to less than 2.8 eV, which indicate the ability of visible light absorption of the composite film for photocatalytic processes. All the bacteria are inactivated under the visible light irradiation in 1 h by using annealed CNTs-doped (20 wt.%) TiO_2 thin lms. In addition, combination of CNTs with other photocatalysts such as ZnO also shows great photoinactivation effect to bacteria [113].

4.4. Antimicrobial, antifouling applications

The antibacterial effect of CNTs based thin films is not limited to CNTs/TiO_2 composite films under the photocatalytic mechanism. Several studies have shown that CNT itself has antimicrobial properties against diverse groups of microorganisms since 2006 [114-117]. SWCNTs are believed to have stronger antimicrobial property than MWCNTs due to a higher aspect ratio and probably some heavy metal residues. Therefore, CNTs based films have been explored as antimicrobial coatings. The antibacterial property of CNTs/polymer composite film was investigated by School *et al.* [118] They tested the effect of SWCNTs/PVK composite films on planktonic cells and biofilms of Escherichia coli and Bacillus subtilis. The results suggested that the SWCNTs/PVK composite film had antibacterial activity on planktonic cells and biofilms at all concentration levels. Qi *et al.* [119,120] demonstrated that immobilization of antimicrobial molecules to MWCNTs via covalent bonding could further improve the antimicrobial activity. They found that the MWCNTs/nisin and MWCNTs/cephalexin composite films exhibited superior antimicrobial and antibiofilm properties.

Antifouling coatings have important application in food industry and medical instruments. Two general routes have been used for fabrication of CNTs based antifouling coatings. One is to coat CNTs onto metal substrates to create superhydrophobic surfaces [121]. As an example, Rungraeng *et al.* [122] reported the successful inhibition of milk foulant by applying the superhydrophobic CNTs/polytetrafluoroethylene (PTFE) coating on the surface of the plate heat exchanger. Results indicated that after milk pasteurization for 5 h, the mass of foulant on CNTs/PTFE coated heat exchanger surface was 70.3% less than that on the uncoated surface. The total energy consumption of testing PHE unit also dropped by 10.2%. Another method is to form CNTs/enzyme/polymer composite films. In this system, CNTs contribute large surface area to load large amount of enzymes and the high aspect ratio of CNT helps to retain CNTs/enzyme conjugates in the matrix. The rate of enzyme proteolysis was greatly improved, which leads to the elimination of surface biofouling. Furthermore, CNTs could also enhance the stability of adsorbed proteins [123].

5. SUMMARY AND PERSPECTIVE

Although CNTs were discovered over a decade ago, the progress of preparation and application of CNTs based thin films was initially hindered by the high cost. Recent innovations in experimental techniques have greatly advanced the development of these films. Achievements on synthesis, characterization, and device applications of CNTs based thin films. These films can be fabrication by various techniques, each technique described here has its own advantage and disadvantage. Nevertheless, large-scale preparation of CNTs films, accurately controlling the size and thickness and longterm stability are still challenges for future research. Furthermore, some drawbacks of the fabrication process such as the high temperature requirement of CVD method, long time process of LbL selfassembly method could restrict the practical implementation of these techniques. It is also noted that some techniques described here still remain at the proof-of-principle stage.

The advanced characterization techniques described in this review are used not only for characterizing the property of the sample but also as the competent tools for monitoring the fabrication process. Through results comparison and fabrication process adjustment, the relationship between the primary properties, film processing condition and device performance could be established. Using different techniques allows researchers to complement different results and build up a full understanding of the film.

The applications of CNTs based thin films are multidisciplinary. Among them, CNTs/polymer composite films have been the most widely studied, ranging from small electronic devices to large antifouling films. Recently, CNTs/photocatalyst composite films also attract enormous attention. However,

few applications have yet been advanced to the production. In addition to the shortage of mature fabrication techniques, lack of full knowledge on the photocatalytic mechanism is also a roadblock to accelerate the extensive application. For instance, while enhanced photocatalysis of CNTs/TiO_2 composites has been achieved for the degradation organic pollutants in wastewater and air, the mechanism of synergic effect of CNTs on TiO_2 photocatalytic activity is still unclear. Ultimately, the use of CNTs based thin film represents a challenging but potentially a rewarding opportunity to develop the next generation of advanced functional materials.

ACKNOWLEDGMENTS

The work is partially supported by the National Natural Science Foundation of China (Grant number: 21075030).

REFERENCES

[1] P.M. Ajayan // *Chemical Reviews* **99** (1999) 1787.
[2] Q. Zhao, Z. Gan and Q. Zhuang // *Electroanalysis* **14** (2002) 1609.
[3] K. Balasubramanian and M. Burghard // *Small* **1** (2005) 180.
[4] M.M.J. Treacy, T.W. Ebbesen and J.M. Gibson // *Nature* **381** (1996) 678.
[5] E.W. Wong, P.E. Sheehan and C.M. Lieber // *Science* **277** (1997) 1971.
[6] H. Dai, E.W. Wong and C.M. Lieber // *Science* **272** (1996) 523.
[7] E. Pop, D. Mann, Q. Wang, K. Goodson and H. Dai // *Nano Letters* **6** (2006) 96.
[8] H. Huang, C. Liu, Y. Wu and S. Fan // *Advanced Materials* **17** (2005) 1652.
[9] A.E. Aliev, J. Oh, M.E. Kozlov, A.A. Kuznetsov, S. Fang, A.F. Fonseca, R. Ovalle, M.D. Lima, M.H. Haque, Y.N. Gartstein, M. Zhang, A.A. Zakhidov and R.H. Baughman // *Science* **323** (2009) 1575.
[10] L. Qu, L. Dai, M. Stone, Z. Xia and L.W. Zhong // *Science* **322** (2008) 238.
[11] B. Yurdumakan, N.R. Raravikar, P.M. Ajayan and A. Dhinojwala // *Chemical Communications* **30** (2005) 3799.
[12] E. Ramasamy, W.J. Lee, D.Y. Lee and J.S. Song // *Electrochemistry Communications* **10** (2008) 1087.
[13] A. Schindler, J. Brill, N. Fruehauf, J.P. Novak and Z. Yaniv // *Physica E: Low-Dimensional Systems and Nanostructures* **37** (2007) 119.
[14] M. Jeong, K. Lee, E. Choi, A. Kim and S.B. Lee // *Nanotechnology* **23** (2012) 505203.
[15] Y. Li, T. Yu, T. Pui, P. Chen, L. Zheng and K. Liao // *Nanoscale* **3** (2011) 2469.
[16] V. Bliznyuk, S. Singamaneni, R. Kattumenu and M. Atashbar // *Applied Physics Letters* **88** (2006).
[17] S.H. Lee, H.T. Ham, J.S. Park, I.J. Chung and S.O. Kim // *Macromolecular Symposia* **249-250** (2007) 618.
[18] B. Safadi, R. Andrews and E.A. Grulke // *Journal of Applied Polymer Science* **84** (2002) 2660.
[19] W. Ding, V. Koutsos, I. Si and Z. Song // *Advanced Materials Research* **569**, (2012) 15.
[20] J.H. Yim, Y.S. Kim, K.H. Koh and S. Lee // *Journal of Vacuum Science and Technology B: Microelectronics and Nanometer Structures* **26** (2008) 851.
[21] M.A. Meitl, Y. Zhou, A. Gaur, S. Jeon, M.L. Usrey, M.S. Strano and J.A. Rogers // *Nano Letters* **4** (2004) 1643.
[22] J.W. Jo, J.W. Jung, J.U. Lee and W.H. Jo // *ACS Nano* **4** (2010) 5382.
[23] L. Berguiga, J. Bellessa, F. Vocanson, E. Bernstein and J.C. Plenet // *Optical Materials* **28** (2006) 167.
[24] E.R. Morales, N.R. Mathews, D. Reyes-Coronado, C.R. Magańa, D.R. Acosta, G. Alonso-Nunez, O.S. Martinez and X. Mathew // *Solar Energy* **86** (2012) 1037.
[25] W. Wang, P. Serp, P. Kalck and J.L. Faria // *Journal of Molecular Catalysis A: Chemical* **235** (2005) 194.
[26] J.S. Lee, T.J. Ha, M.H. Hong, C.S. Park and H.H. Park // *Applied Surface Science* **269** (2013) 125.
[27] S. Sharma, S. Hussain, K. Sengupta and S.S. Islam // *Applied Physics A: Materials Science and Processing* **111** (2012) 965.
[28] K.T. Roro, N. Tile, B. Mwakikunga, B. Yalisi and A. Forbes // *Materials Science and Engineering: B* **177** (2012) 581.
[29] C.K. Lin, S.C. Tseng, C.H. Cheng, C.Y. Chen and C.C. Chen // *Thin Solid Films* **520** (2011) 1375.
[30] C. Luo, X. Zuo, L. Wang, E. Wang, S. Song, J. Wang, C. Fan and Y. Cao // *Nano Letters* **8** (2008) 4454.
[31] H. Yao, C.C. Chu, H.J. Sue and R. Nishimura // *Carbon* **53** (2013) 366.

[32] C. Du, D. Heldbrant and N. Pan // *Materials Letters* **57** (2002) 434.
[33] J. Zhang, Y. Wang, J. Zang, G. Xin, Y. Yuan and X. Qu // *Carbon* **50** (2012) 5196.
[34] B. Gao, G.Z. Yue, Q. Qiu, Y. Cheng, H. Shimoda, L. Fleming and O. Zhou // *Advanced Materials* **13** (2001) 1770.
[35] F. Su, C. Liu, J. Guo and P. Huang // *Surface and Coatings Technology* **217** (2013) 94.
[36] H.M. Wu, P.F. Hsu and W.T. Hung // *Diamond and Related Materials* **18** (2009) 337.
[37] A. Yu, Q. Wang, J. Yong, P.J. Mahon, F. Malherbe, F. Wang, H. Zhang and J. Wang // *Electrochimica Acta* **74** (2012) 111.
[38] N. Alexeyeva, J. Kozlova, V. Sammelselg, P. Ritslaid, H. Mändar and K. Tammeveski // *Applied Surface Science* **256** (2010) 3040.
[39] L. Tammeveski, H. Erikson, A. Sarapuu, J. Kozlova, P. Ritslaid, V. Sammelselg and K. Tammeveski // *Electrochemistry Communications* **20** (2012) 15.
[40] Z. Tang, H.Y. Ng, J. Lin, A.T.S. Wee and D.H.C. Chua // *Journal of the Electrochemical Society* **157** (2010) B245.
[41] K.S. Lee and D.M. Kim // *International Journal of Hydrogen Energy* **37** (2012) 6272.
[42] F. Jin, Y. Liu and C.M. Day, In: *Vacuum Electronics Conference, 2007. IVEC '07. IEEE International* (IEEE, 2007), p. 1.
[43] C.C. Chang and C.C. Chen, In: *Technical Proceedings of the 2006 NSTI Nanotechnology Conference and Trade Show* (2006), p.17.
[44] A. Yu, X. Zhang, H. Zhang, D. Han and A.R. Knight // *Electrochimica Acta* **56** (2011) 9015.
[45] A. Yu // *Chemistry Letters* **41** (2012) 1492.
[46] H.-L. Wang, J. Liu and D.-J. Qian // *Synthetic Metals* **162** (2012) 881.
[47] C.E. Hamilton, J.R. Lomeda, Z. Sun, J.M. Tour and A.R. Barron // *Nano Letters* **9** (2009) 3460.
[48] A. Aguilar-Elguézabal, W. Antúnez, G. Alonso, F.P. Delgado, F. Espinosa and M. Miki-Yoshida // *Diamond and Related Materials* **15** (2006) 1329.
[49] R. Xiang, Z. Yang, Q. Zhang, G. Luo, W. Qian, F. Wei, M. Kadowaki, E. Einarsson and S. Maruyama // *Journal of Physical Chemistry C* **112** (2008) 4892.
[50] J. Su, Y. Yu and R.C. Che // *Applied Physics A: Materials Science and Processing* **90** (2008) 135.
[51] X. Dong, B. Li, A. Wei, X. Cao, M.B. Chan-Park, H. Zhang, L.J. Li, W. Huang and P. Chen // *Carbon* **49** (2011) 2944.
[52] Y.S. Li, T.J. Pan, Y. Tang, Q. Yang and A. Hirose // *Diamond and Related Materials* **20** (2011) 187.
[53] R. Epur, M.K. Datta and P.N. Kumta // *Electrochimica Acta* **85** (2012) 680.
[54] L. Marot, T. de los Arcos, A.M. Bünzli, C. Wäckerlin, R. Steiner, P. Oelhafen, E. Meyer, D. Mathys, P. Spätig and G. Covarel // *Surface and Coatings Technology* **212** (2012) 223.
[55] J.S. Park, J.P. Kim, Y.R. Noh, K.C. Jo, S.Y. Lee, H.Y. Choi and J.U. Kim // *Thin Solid Films* **519** (2010) 1743.
[56] F. Huakang, D. Miao and Z. Qiang // *ACS Applied Materials and Interfaces* **4** (2012) 1981.
[57] Y. Zhang, H. Ma, K. Zhang, S. Zhang and J. Wang // *Electrochimica Acta* **54** (2009) 2385.
[58] T. Sawatsuk, A. Chindaduang, C. Sae-kung, S. Pratontep and G. Tumcharern // *Diamond and Related Materials* **18** (2009) 524.
[59] L. Li, G. Zhang, L. Chen, H.-M. Bi and K.-Y. Shi // *Materials Research Bulletin* **48** (2013) 504.
[60] K. Li, C. Zhang, Z. Du, H. Li and W. Zou // *Synthetic Metals* **162** (2012) 2010.
[61] C. Villeneuve, S. Pacchini, P. Boulanger, A. Brouzes, F. Roussel, M. Pinault, M. Mayne-L'Hermite and R. Plana // *Journal of Applied Physics* **112** (2012).
[62] T. Belin and F. Epron // *Materials Science and Engineering: B* **119** (2005) 105.
[63] B. Ghaddab, J.B. Sanchez, C. Mavon, M. Paillet, R. Parret, A.A. Zahab, J.L. Bantignies, V. Flaud, E. Beche and F. Berger // *Sensors and Actuators B: Chemical* **170** (2012) 67.
[64] W. Du, F. Zhao and B. Zeng // *Journal of Chromatography A* **1216** (2009) 3751.
[65] S. Quillard, G. Louarn, S. Lefrant and A.G. Macdiarmid // *Physical Review B* **50** (1994) 12496.
[66] M. Baibarac, I. Baltog, S. Lefrant, J.Y. Mevellec and O. Chauvet // *Chemistry of Materials* **15** (2003) 4149.
[67] C. Basavaraja, E.A. Jo, B.S. Kim and D.S. Huh // *Polymer Composites* **32** (2011) 438.
[68] G. Wei, J. Zhang, L. Xie and K.D. Jandt // *Carbon* **49** (2011) 2216.

[69] K.M. Cui, M.C. Tria, R. Pernites, C.A. Binag and R.C. Advincula // *ACS Applied Materials & Interfaces* **3** (2011) 2300.
[70] A. Maity, S.S. Ray and S.K. Pillai // *Macromolecular Rapid Communications* **28** (2007) 2224.
[71] Z. Li, B. Gao, G.Z. Chen, R. Mokaya, S. Sotiropoulos and G. Li Puma // *Applied Catalysis B: Environmental* **110** (2011) 50.
[72] M. Sánchez and M.E. Rincón // *Sensors and Actuators B: Chemical* **140** (2009) 17.
[73] G. Aridoss, M.S. Kim, S.M. Son, J.T. Kim and Y.T. Jeong // *Polymers for Advanced Technologies* **21** (2010) 881.
[74] J.-B. Kim, J.-W. Yi and J.-E. Nam // *Thin Solid Films* **519** (2011) 5050.
[75] C. Peng, J. Jin and G.Z. Chen // *Electrochimica Acta* **53** (2007) 525.
[76] Y. Liu, Y. Liu, H. Feng, Y. Wu, L. Joshi, X. Zeng and J. Li // *Biosensors and Bioelectronics* **35** (2012) 63.
[77] C. Dhand, S.K. Arya, S.P. Singh, B.P. Singh, M. Datta and B.D. Malhotra // *Carbon* **46** (2008) 1727.
[78] M. Saleem, K.S. Karimov and Z.M. Karieva // *A. Mateen, Physica E: Low-dimensional Systems and Nanostructures* **43** (2010) 28.
[79] M. Shah, Z. Ahmad, K. Sulaiman, K.S. Karimov and M.H. Sayyad // *Solid-State Electronics* **69** (2012) 18.
[80] L. Liu, X. Ye, K. Wu, Z. Zhou, D. Lee and T. Cui // *IEEE Sensors Journal* **9** (2009) 1308.
[81] H. Yu, T. Cao, L. Zhou, E. Gu, D. Yu and D. Jiang // *Sensors and Actuators B: Chemical* **119** (2006) 512.
[82] H. Jing, Y. Jiang, X. Du, H. Tai and G. Xie // *Applied Physics A: Materials Science and Processing* **109** (2012) 111.
[83] A.L. Friedman, H. Chun, D. Heiman, Y. Joon Jung and L. Menon // *Physica B: Condensed Matter* **406** (2011) 841.
[84] K.H.S. Karimov, F.A. Khalid, M. Tariq Saeed Chani, A. Mateen, M. Asif Hussain and A. Maqbool // *Optoelectronics and Advanced Materials, Rapid Communications* **6** (2012) 194.
[85] N. Inomata and F. Arai // *Japanese Journal of Applied Physics* **50** (2011).
[86] K.S. Karimov, M.T.S. Chani and F.A. Khalid // *Physica E: Low-dimensional Systems and Nanostructures* **43** (2011) 1701.
[87] A. Saraiya, D. Porwal, A.N. Bajpai, N.K. Tripathi and K. Ram // *Synthesis and Reactivity in Inorganic, Metal-Organic and Nano-Metal Chemistry* **36** (2006) 163.
[88] C. Cantalini, L. Valentini, I. Armentano, J.M. Kenny, L. Lozzi and S. Santucci // *Journal of the European Ceramic Society* **24** (2004) 1405.
[89] J.-H. Lee, J. Kim, H.W. Seo, J.-W. Song, E.-S. Lee, M. Won and C.-S. Han // *Sensors and Actuators B: Chemical* **129** (2008) 628.
[90] X. Liu, S. Cheng, H. Liu, S. Hu, D. Zhang and H. Ning // *Sensors (Switzerland)* **12** (2012) 9635.
[91] K. Seong-Jeen // *Sensors Journal, IEEE* **10** (2010) 173.
[92] W. Lin, S. Huang and W. Chen // *Journal of Semiconductors* **31** (2010) 024006.
[93] L. Valentini, V. Bavastrello, E. Stura, I. Armentano, C. Nicolini and J.M. Kenny // *Chemical Physics Letters* **383** (2004) 617.
[94] J. Li, Y. Lu, Q. Ye, M. Cinke, J. Han and M. Meyyappan // *Nano Letters* **3** (2003) 929.
[95] L. Valentini, F. Mercuri, I. Armentano, C. Cantalini, S. Picozzi, L. Lozzi, S. Santucci, A. Sgamellotti and J.M. Kenny // *Chemical Physics Letters* **387** (2004) 356.
[96] F. Patolsky, Y. Weizmann and I. Willner // *Angewandte Chemie - International Edition* **43** (2004) 2113.
[97] C. Ou, R. Yuan, Y. Chai, M. Tang, R. Chai and X. He // *Analytica Chimica Acta* **603** (2007) 205.
[98] X. Qin, H. Wang, X. Wang, S. Li, Z. Miao, N. Huang and Q. Chen // *Materials Science and Engineering: C* **29** (2009) 1453.
[99] C.W. Tan, K.H. Tan, Y.T. Ong, A.R. Mohamed, S.H.S. Zein and S.H. Tan // *Environmental Chemistry Letters* **10** (2012) 265.
[100] C. Klinger, Y. Patel and H.W.C. Postma // *PLoS ONE* **7** (2012).
[101] B.K. Koo, D.Y. Lee, H.J. Kim, W.J. Lee and J.S. Song // *Journal of Electroceramics* **17** (2006) 79.
[102] J.E. Trancik, S.C. Barton and J. Hone // *Nano Letters* **8** (2008) 982.
[103] S. Hwang, J. Moon, S. Lee, D.H. Kim, D. Lee, W. Choi and M. Jeon // *Electronics Letters* **43** (2007) 1455.
[104] A. Kongkanand, S. Kuwabata, G. Girishkumar and P. Kamat // *Langmuir* **22** (2006) 2392.
[105] K. Stolarczyk, M. Sepelowska, D. Lyp, K. Żelechowska, J.F. Biernat, J. Rogalski,

K.D. Farmer, K.N. Roberts and R. Bilewicz // *Bioelectrochemistry* **87** (2012) 154.
[106] M. Holzinger, A. Le Goff and S. Cosnier // *Electrochimica Acta* **82** (2012) 179.
[107] L. Deng, L. Shang, Y. Wang, T. Wang, H. Chen and S. Dong, // *Electrochemistry Communications* **10** (2008) 1012.
[108] A. Kozinda, Y. Jiang and L. Lin, In: *Micro Electro Mechanical Systems (MEMS), 2012 IEEE 25th International Conference on* (IEEE, 2012), p. 1233.
[109] J. Zhang, L.-B. Kong, B. Wang, Y.-C. Luo and L. Kang // *Synthetic Metals* **159** (2009) 260.
[110] M.R. Hoffmann, S.T. Martin, W. Choi and D.W. Bahnemann // *Chemical Reviews* **95** (1995) 69.
[111] K.E. Tettey, M.Q. Yee and D. Lee // *ACS Applied Materials & Interfaces* **2** (2010) 2646.
[112] O. Akhavan, R. Azimirad, S. Safa and M.M. Larijani // *Journal of Materials Chemistry* **20** (2010) 7386.
[113] O. Akhavan, R. Azimirad and S. Safa // *Materials Chemistry and Physics* **130** (2011) 598.
[114] T. Akasaka and F. Watari // *Acta Biomaterialia* 5 (2009) 607.
[115] S. Kang, M.S. Mauterv M. Elimelech // *Environmental Science and Technology* **42** (2008) 7528.
[116] D. Nepal, S. Balasubramanian, A.L. Simonian and V.A. Davis // *Nano Letters* **8** (2008) 1896.
[117] Z. Ying, R. Tiecheng, L. Yuguo, G. Jinxue and L. Wenxin // *Nanotechnology* **17** (2006) 4668.
[118] F. Ahmed, C.M. Santos, R.A.M.V. Vergara, M.C.R. Tria, R. Advincula and D.F. Rodrigues // *Environmental Science & Technology* **46** (2011) 1804.
[119] X. Qi, G. Poernomo, K. Wang, Y. Chen, M.B. Chan-Park, R. Xu and M.W. Chang // *Nanoscale* **3** (2011) 1874.
[120] X. Qi, P. Gunawan, R. Xu and M.W. Chang // *Chemical Engineering Science* **84** (2012) 552.
[121] X.-H. Men, Z.-Z. Zhang, J. Yang, K. Wang and W. Jiang // *Applied Physics A* **98** (2010) 275.
[122] N. Rungraeng, Y.-C. Cho, S.H. Yoon and S. Jun // *Journal of Food Engineering* **111** (2012) 218.
[123] P. Asuri, S.S. Karajanagi, R.S. Kane and J.S. Dordick // *Small* **3** (2007) 50.
[124] Z. Cao and B. Wei // *Nano Energy* Impress (2012).
[125] X. Li and B. Wei // *Nano Energy* **1** (2012) 479.
[126] B.-R. Huang and T.-C. Lin // *International Journal of Hydrogen Energy* **36** (2011) 15919.
[127] Y. Battie, O. Ducloux, P. Thobois, T. Susi, E.I. Kauppinen and A. Loiseau // *Physica Status Solidi (B) Basic Research* **248** (2011) 2462.
[128] D. Zilli, P.R. Bonelli and A.L. Cukierman // *Sensors and Actuators B: Chemical* **157** (2011) 169.
[129] H.Y. Jeong, D.S. Lee, H.K. Choi, D.H. Lee, J.E. Kim, J.Y. Lee, W.J. Lee, S.O. Kim and S.Y. Choi // *Applied Physics Letters* **96** (2010).
[130] M. Raghu, R. Suresh and P.S. Vijay // *Nanotechnology* **22** (2011) 215502.
[131] W. Changbao, Z. Changchun, J. Yongfeng, L. Li, L. Wanlin, Y. Dong, X. Hongke and Q. Yanzhang // *Smart Materials and Structures* **20** (2011) 035006.
[132] P.-G. Su and T.-T. Pan // *Materials Chemistry and Physics* ***1*25** (2011) 351.
[133] B.A. Albiss, W.A. Sakhaneh, I. Jumah and I.M. Obaidat // *IEEE Sensors Journal* **10** (2010) 1807.